Supplement of Atmos. Chem. Phys., 23, 15671–15691, 2023
https://doi.org/10.5194/acp-23-15671-2023-supplement

Atmospheric Chemistry and Physics
Open Access
EGU

Supplement of

Examining the vertical heterogeneity of aerosols over the Southern Great Plains

Yang Wang et al.

Correspondence to: Yang Wang (yangwang@miami.edu)

Fig. S1. Satellite imagery showing the terrain and vegetation surrounding the SGP observatory. Map is obtained from ©Google Maps.

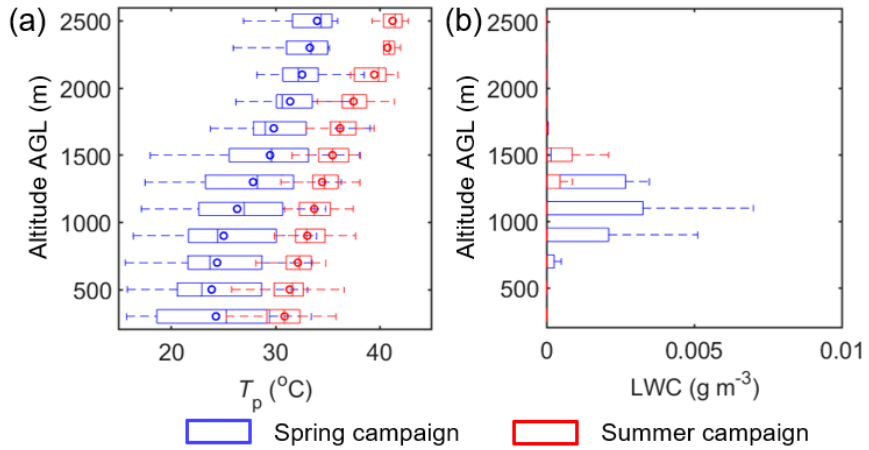

Fig. S2. Vertical profiles of (a) potential temperature (T_p) and (b) liquid water content (LWC) during the spring and summer campaigns.

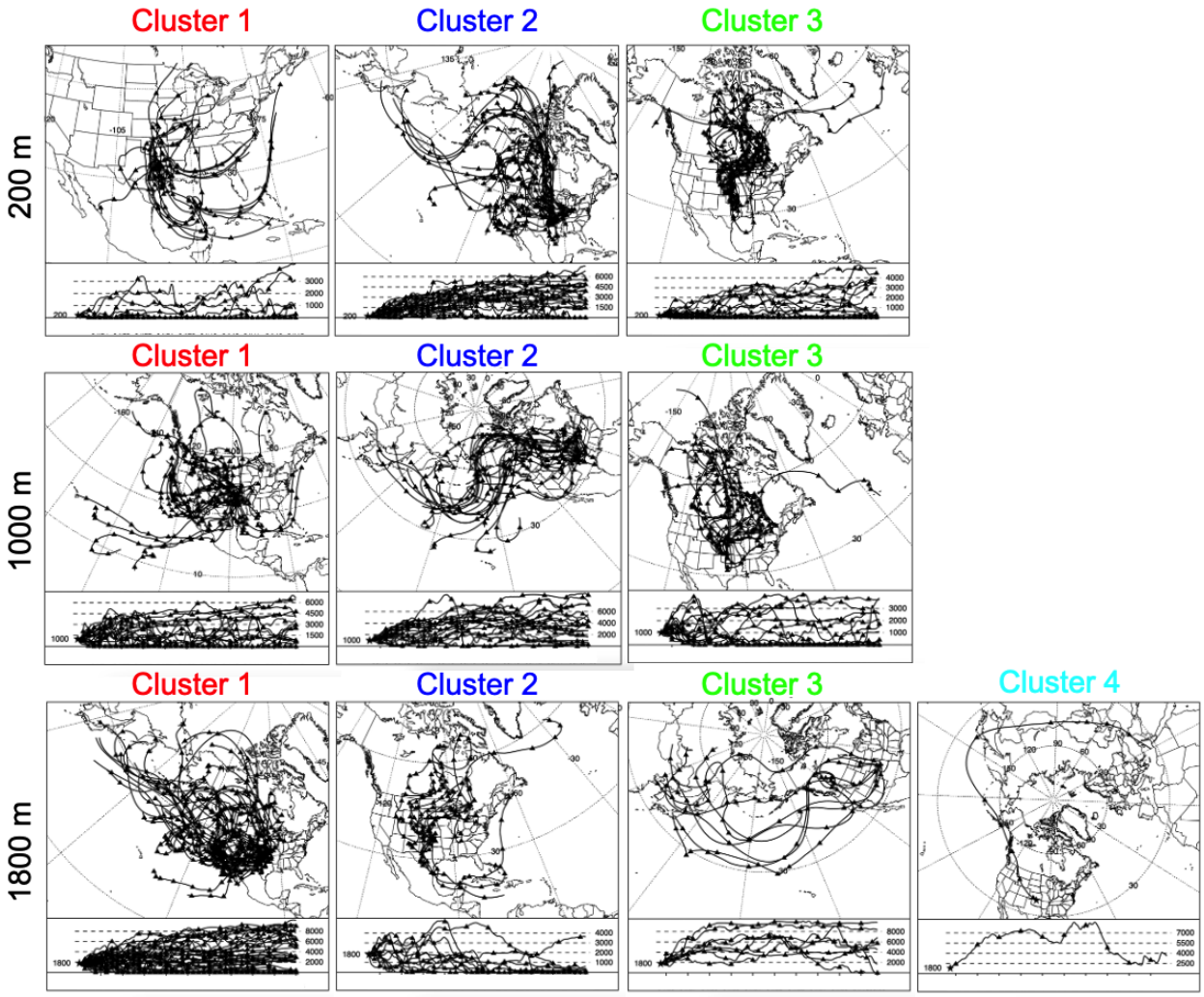

Fig. S3. Trajectories associated with each cluster during the spring campaign shown in Fig. 3.

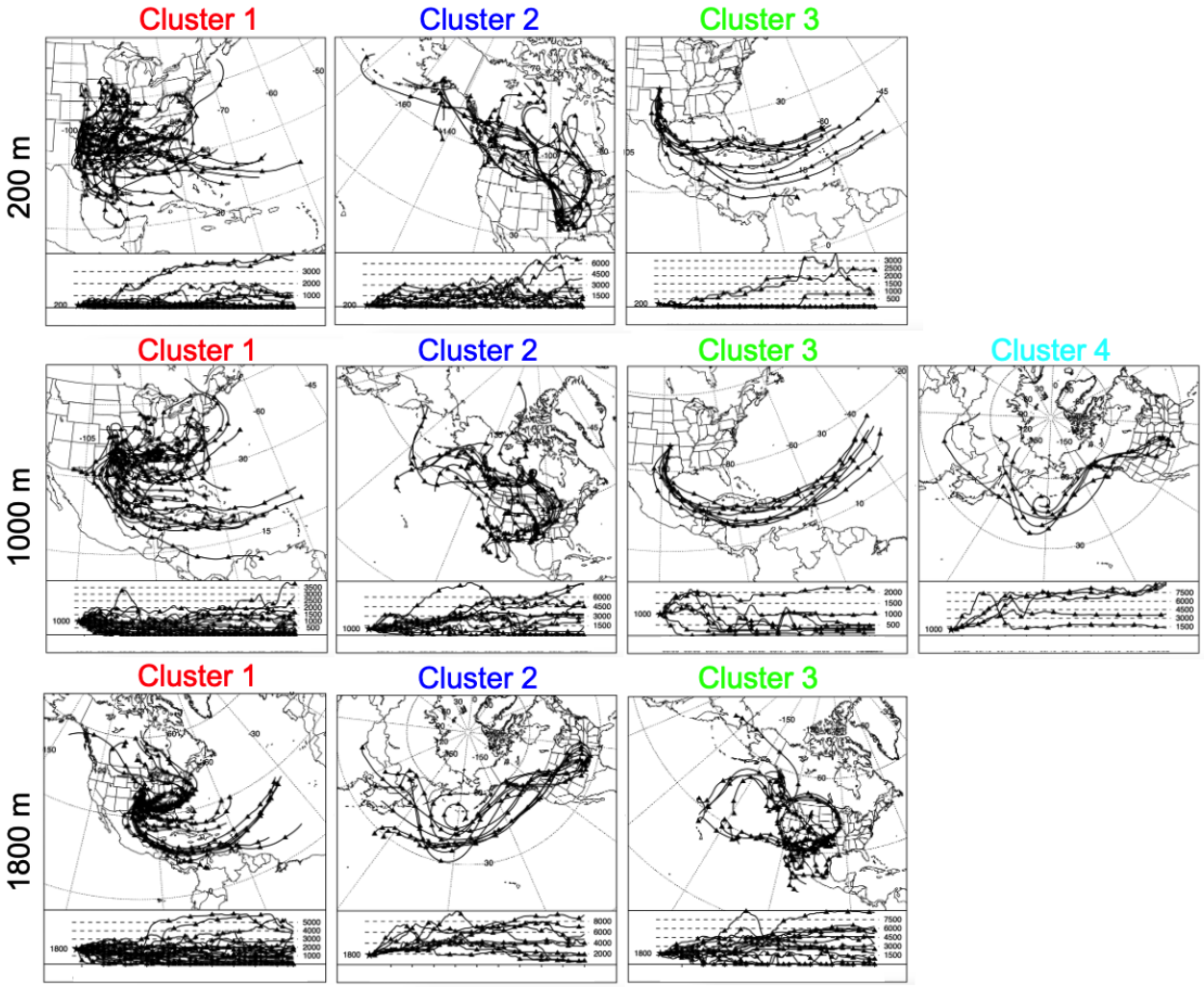

Fig. S4. Trajectories associated with each cluster during the summer campaign shown in Fig. 3.

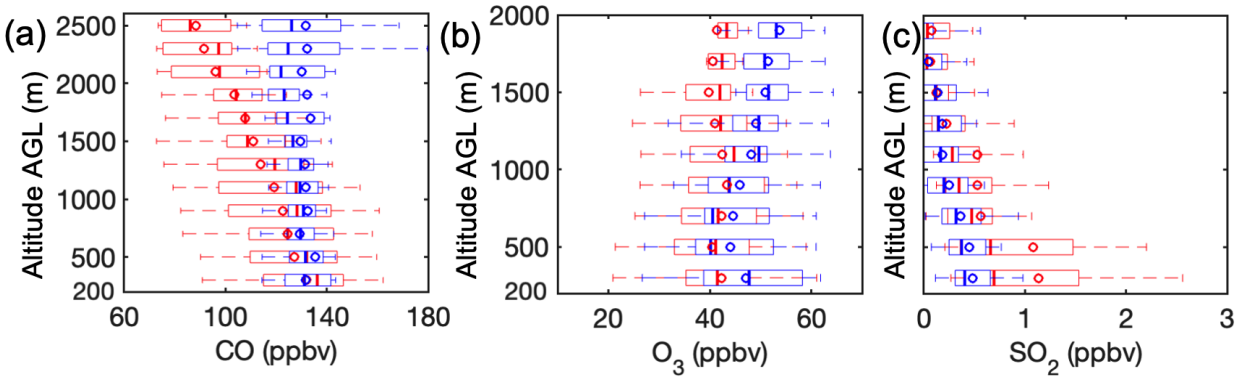

Fig. S5. Vertical profiles of (a) carbon monoxide mixing ratio (CO), (b) ozone mixing ratio (O_3), and (c) sulfur dioxide mixing ratio (SO_2) over the SGP site during the spring IOP (blue) and summer IOP (red). The line and circle markers represent the median and mean concentrations, and the edges of the box indicate the 25th and 75th percentiles, respectively. Note that different altitude ranges are used: CO was reported from 200 to 2500 m, and O_3 and SO_2 are reported from 200 to 2000 m. SO_2 mixing ratio for each flight is corrected by a constant offset so that the minimum mixing ratio value is set to 0.

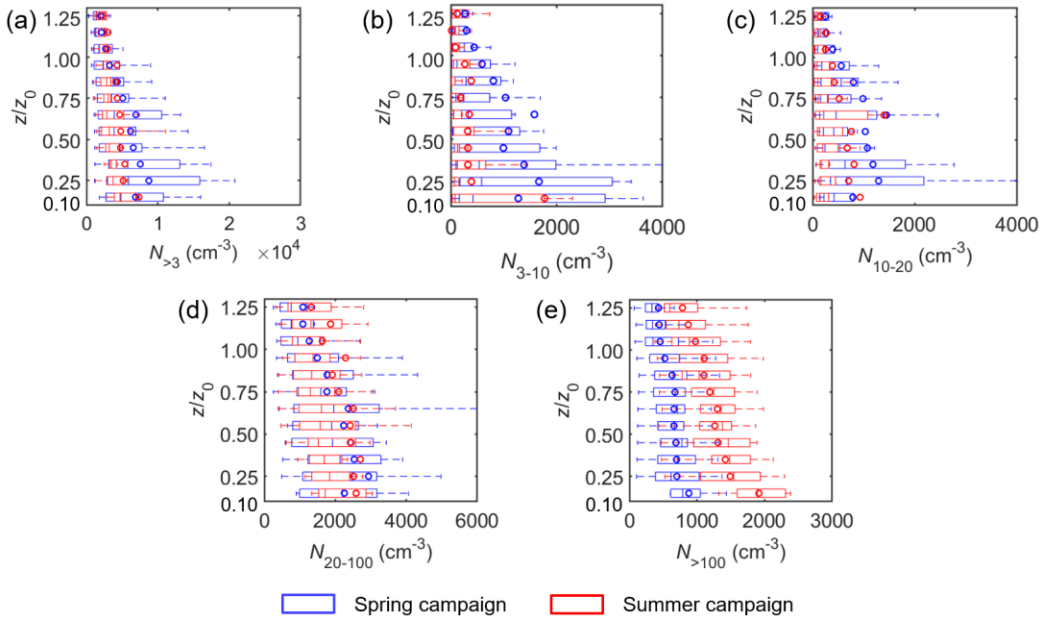

Fig. S6. Vertical profiles (against normalized altitude) showing the concentrations of particles (a) larger than 3 nm ($N_{>3}$), (b) with sizes between 3 and 10 nm ($N_{3\text{-}10}$), (c) with sizes between 10 and 20 nm ($N_{10\text{-}20}$), (d) with sizes between 20 and 100 nm ($N_{20\text{-}100}$), (e) with sizes above 100 nm ($N_{>100}$) over the SGP site during the spring campaign (blue) and summer campaign (red). The altitude is normalized against the boundary layer height for each flight. The line and circle markers represent the median and mean of the data, and the edges of the box indicate the 25th and 75th percentiles, respectively. The concentrations are normalized to standard temperature and pressure (273.15 K and 101.325 kPa; STP).

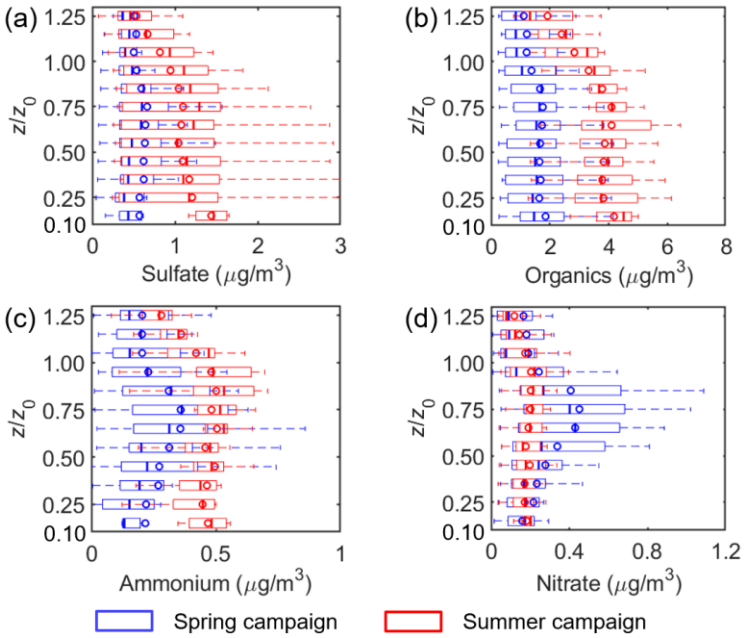

Fig. S7. Vertical profiles (against normalized altitude) of the mass concentrations of (a) sulfate, (b) organics, (c) ammonium, and (d) nitrate over the SGP during the spring IOP (blue) and summer IOP (red). The altitude is normalized against the boundary layer height for each flight. The compositions are measured by the HR-ToF-AMS. The concentration of chloride is too low, and therefore, is not shown in the figure. The line and circle markers represent the median and mean of the data, and the edges of the box indicate the 25th and 75th percentiles, respectively. The concentrations are normalized to standard temperature and pressure (273.15 K and 101.325 kPa; STP).

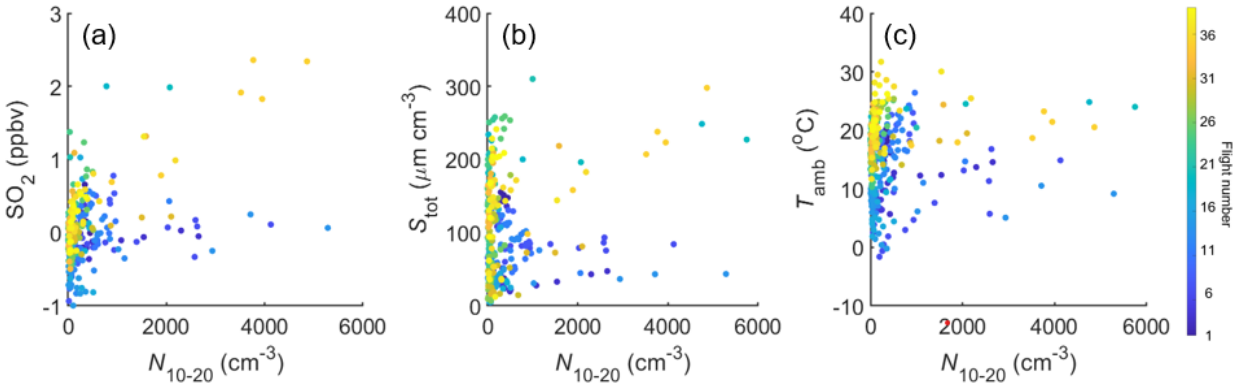

Fig. S8. (a) Correlation between SO_2 mixing ratio and the concentration of aerosols between 10 and 20 nm. (b) Correlation between total aerosol surface area concentration and the concentration of aerosols between 10 and 20 nm. (c) Correlation between ambient temperature and the concentration of aerosols between 10 and 20 nm. Note that raw data on SO_2 mixing ratio are reported. Different colors of the data points represent different flight numbers.

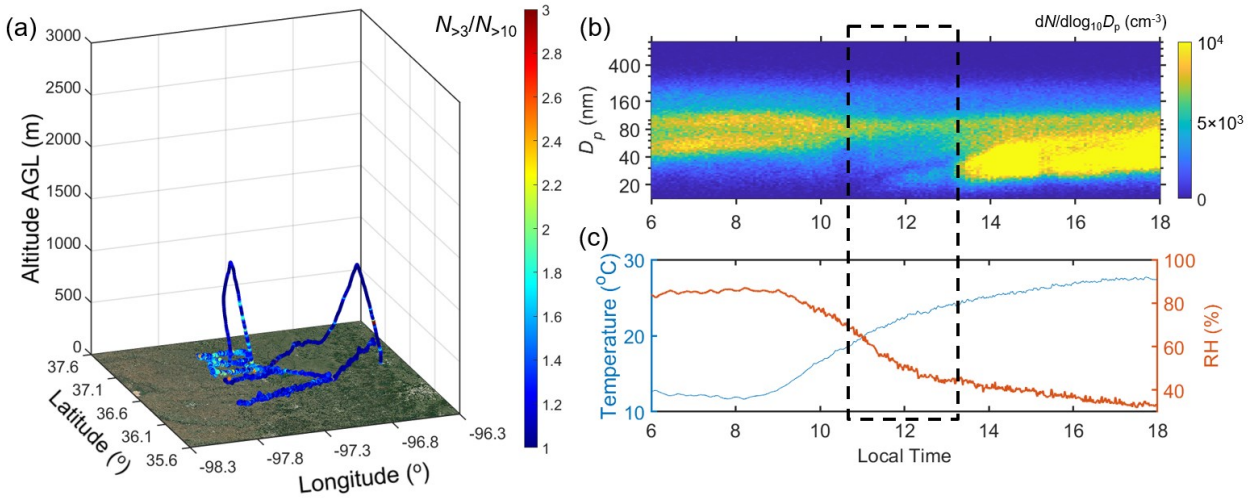

Fig. S9. (a) Track of the G-1 aircraft on September 11, 2016 colored by the ratio between $N_{>3}$ and $N_{>10}$. Map is obtained from ©Google Maps. (b) Aerosol size distribution and (c) temperature and relative humidity (RH) measured at the SGP observatory on September 11, 2016. The dashed box shows the corresponding time for the aircraft measurement.

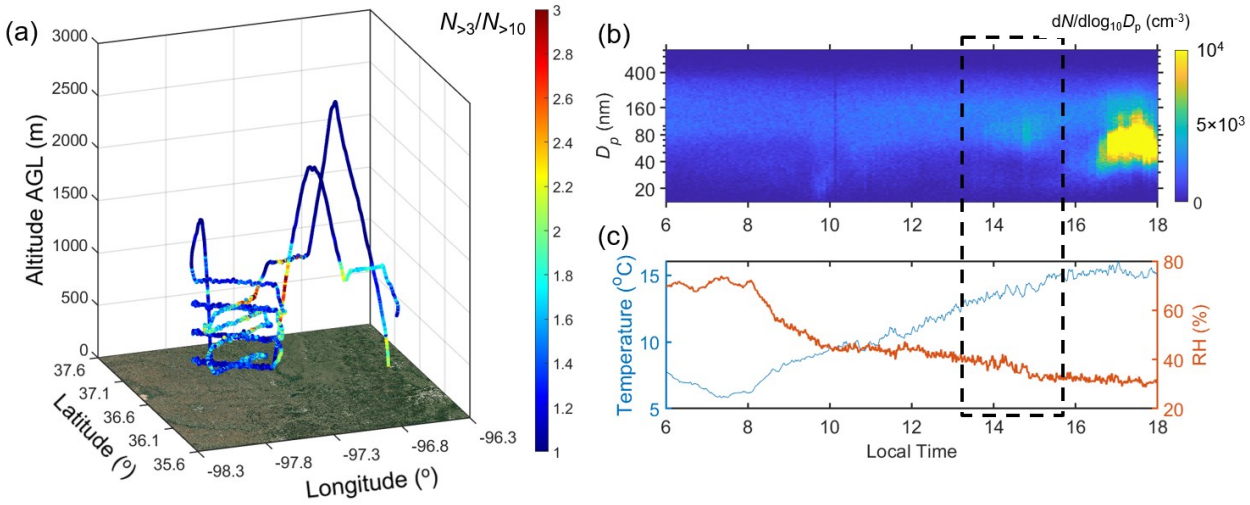

Fig. S10. (a) Track of the G-1 aircraft on May 14, 2016 colored by the ratio between $N_{>3}$ and $N_{>10}$. Map is obtained from ©Google Maps. (b) Aerosol size distribution and (c) temperature and relative humidity (RH) measured at the SGP observatory on May 14, 2016. The dashed box shows the corresponding time for the aircraft measurement.

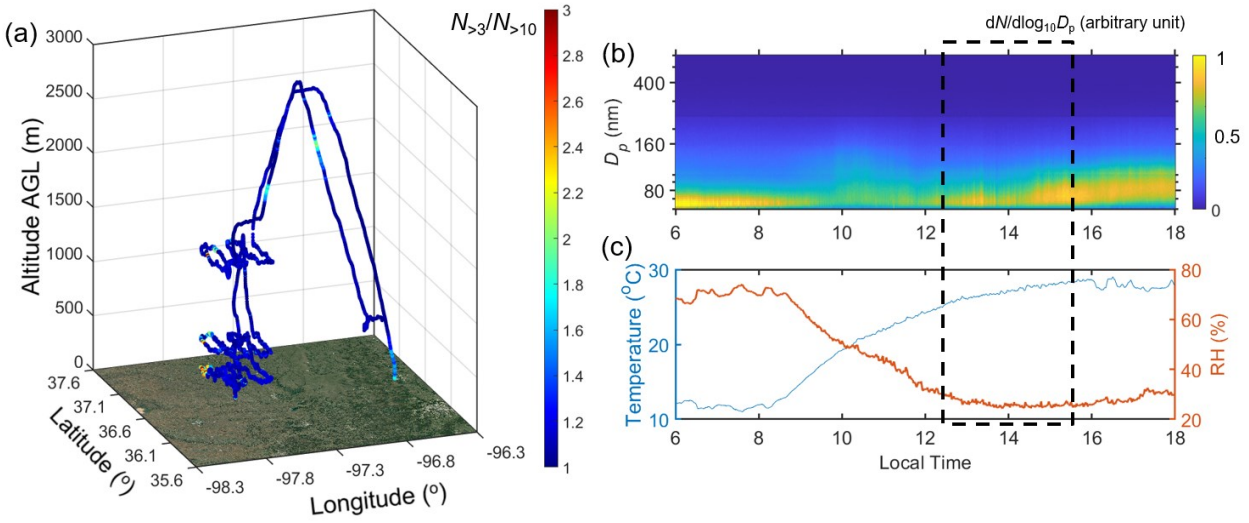

Fig. S11. (a) Track of the G-1 aircraft on May 13, 2016 colored by the ratio between $N_{>3}$ and $N_{>10}$. Map is obtained from ©Google Maps. (b) Aerosol size distribution and (c) temperature and relative humidity (RH) measured at the SGP observatory on May 13, 2016. The dashed box shows the corresponding time for the aircraft measurement.

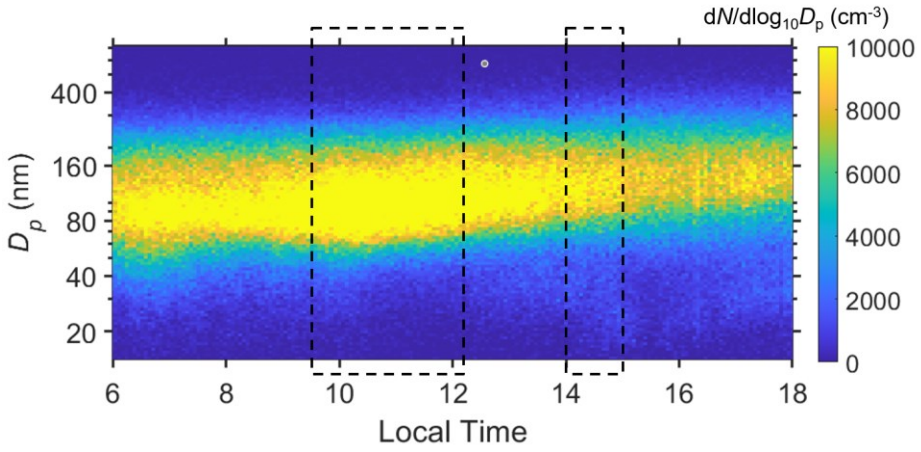

Fig. S12. Aerosol size distribution measured at the SGP observatory on September 4, 2016. The black dashed boxes correspond to morning and afternoon flight times.

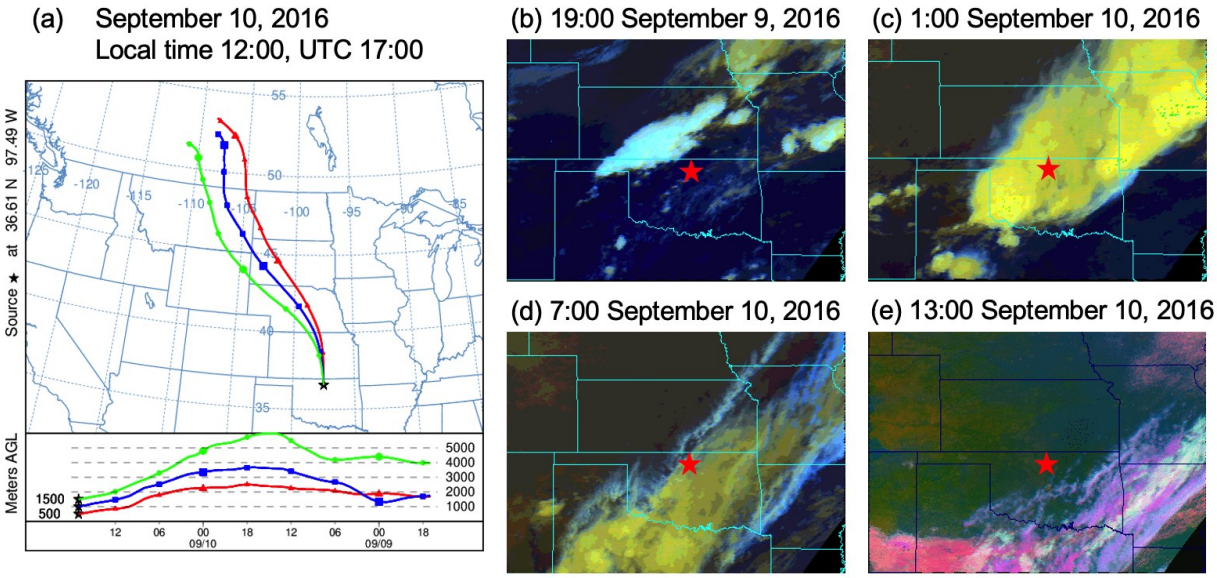

Fig. S13. (a) Back trajectory analysis of air mass arriving at 500, 1000, and 1500 m above the SGP site on September 10, 2016 at local time 12:00 (UTC 17:00), which was in the middle of the aircraft sampling. (b) to (e) Satellite images of clouds above SGP at different local times before and after the deep convective event on September 10, 2016. Satellite imagery is obtained from NASA Satellite Imagery and Cloud Products Page.

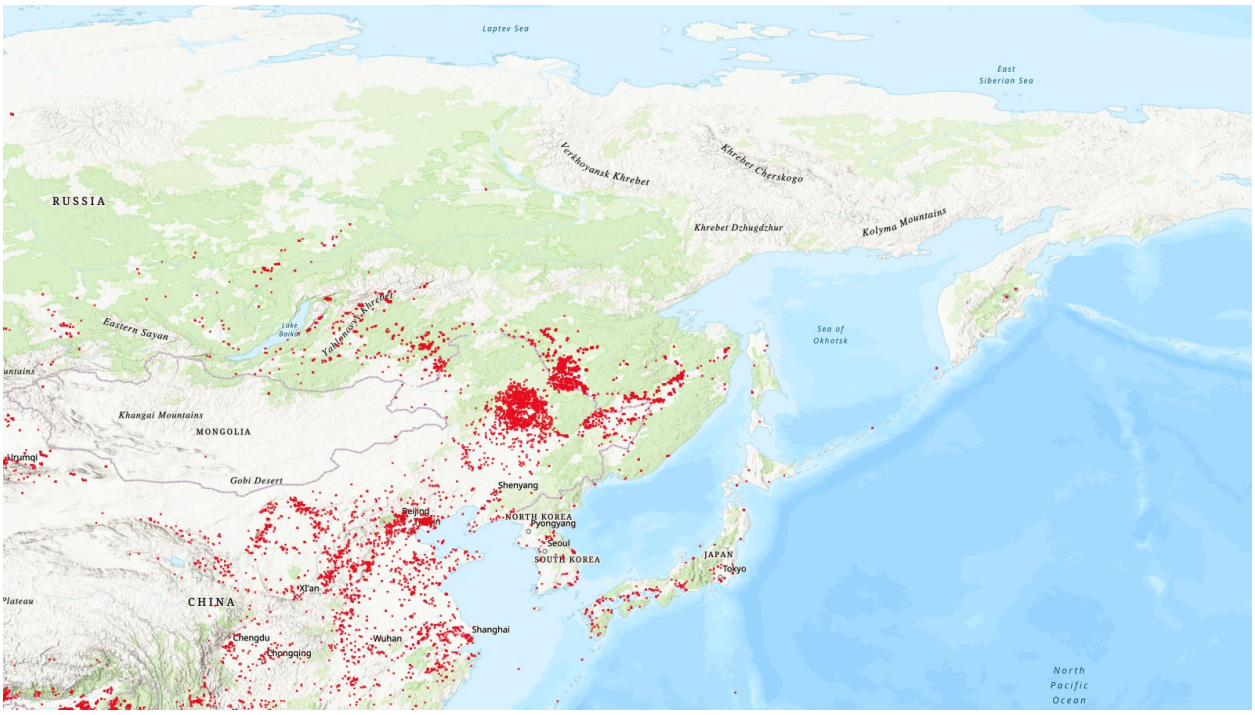

Fig. S14. Fire activities from April 12 to 18, 2016 reported by NASA Fire Information for Resource Management System (FIRMS). Map is created by NASA FIRMS 2023.